

# Umbrella Sampling and UWHAM Methods on a One-Dimensional Brownian Particle

Marcus Schwarting  
meschw04@uchicago.edu

## ABSTRACT

Classical molecular dynamics simulations often fail to fully sample complex systems when a large energy barrier prevents navigating from one potential energy minimum to another. Because free energy computations are strongly linked to complete sampling across the partition function of a system, determining free energy change across various state space positions can be particularly vexing. Many strategies have been devised to tackle this problem. One important approach is umbrella sampling, which partitions a large change across state space into smaller, more manageable bins and limits sampling to this fixed binned region. In this paper, we describe the process of implementing umbrella sampling and demonstrate its efficacy at determining the free energy change across double and triple well potentials on a one-dimensional Brownian particle.

## KEYWORDS

Brownian molecular dynamics, Umbrella sampling, WHAM, MBAR.

### ACM Reference Format:

Marcus Schwarting. 2021. Umbrella Sampling and UWHAM Methods on a One-Dimensional Brownian Particle. In *Proceedings of Molecular Dynamics with Andrew Ferguson*. ACM, New York, NY, USA, 5 pages.

## 1 INTRODUCTION

For a wide array of applications in molecular dynamics (MD) as well as computational chemistry, biology and biochemistry, determining free-energy differences is a critical challenge to determine kinetic spontaneity and energetic equilibria. Umbrella sampling, otherwise known as biased molecular dynamics, is one popular method of providing a free energy approximation along a specified reaction coordinate. Within our framework, biased potentials along a one-dimensional reaction coordinate drive a system from reagent to product through a series of intermediate thermodynamic states. At each intermediate binned state, a full MD simulation is performed. Individual bins can finally be unbiased and combined through a weighted histogram analysis method (WHAM), or a similar unbinned weighted histogram analysis method (UWHAM). This latter UWHAM method, otherwise referred to as multistate Bennet acceptance ratio (MBAR), will be used for unbiasing and aggregating across bins.

## 2 METHODS

In order to derive the free energy of our system, we describe our full process in three main parts. First we detail the underlying dynamics of our selected system, which follows a one-dimensional Brownian particle. Second, we relate the binning and biasing approach undergirding the process of umbrella sampling. Third, we outline the procedure of unbiasing our binned sampling, aggregating using WHAM or UWHAM, and finally determining the Helmholtz free energy of our desired systems.

### 2.1 Langevin and Brownian Dynamics

We will be modelling our simulation after an overdamped Langevin dynamical system, also known as a Brownian dynamical particle [1]. The initial Langevin dynamical equation is of the form

$$M\ddot{X} = -\nabla U(X) - \gamma M\dot{X} + \sqrt{2M\gamma k_B T} R(t)$$

where  $U(X)$  is the potential energy with respect to the position of the particle,  $X(t)$  is the time-dependent position of the particle,  $\dot{X}(t)$  is the time-dependent velocity of the particle,  $\ddot{X}(t)$  is the time-dependent acceleration of the particle,  $M$  is the mass of the particle (which we take to be unity for our experimentation),  $\gamma$  is the damping constant (or friction factor),  $k_B$  is Boltzmann's constant, and  $R(t)$  is a delta-correlated Gaussian process which we will model as

$$R(t) \sim N(0, k_B T / \gamma).$$

Brownian dynamics can be thought of as a special case of the Langevin equation, specifically where no average acceleration takes place (that is,  $\ddot{X} = 0$ ). By also assuming that we are running in a one-dimensional state space, we can rearrange our equation as

$$\frac{dx}{dt} = \frac{1}{\gamma} \frac{dU(x)}{dt} + R(t).$$

Since  $\frac{dU(x)}{dt}$  is equivalent to the magnitude to the force acting on the particle, we now have direct formulation to carry out our full simulation across time steps [2].

At our convenience, we may select a potential energy function across a fixed range of positions, with the caveat that the potential energy surface must be continuously differentiable. We therefore formulate our system as both a double-well potential and a triple well potential. Respectively, these potentials take the forms

$$U_2(x) = \frac{H}{W^4} (x^2 - W^2)^2$$

and

$$U_3(x) = \frac{27H}{4W^6} (x^2 - W^2)^2 (x^2)$$

where  $H$  is the height of the well (typically expressed as a function of  $k_B * T$ ) and  $W$  is half the width between the set of wells (in nm). Note that we could also expand this to include any number of equally deep wells we so chose by using the generalization

$$U_n(x) = C \prod_{k=0}^n \left( x - W + \frac{2Wk}{n} \right)^2$$

where  $C = H/U(x_{max})$  with  $U(x_{max}) \neq 0$  and  $x_{max}$  being any nontrivial solution to the equation

$$0 = \sum_{k=0}^n \left[ \prod_{j \neq k} \left( x - W + \frac{2Wj}{n} \right) \right].$$

By varying  $H$  and  $W$  across some set range, we can experiment across a wide set of double-well and triple-well potential energy

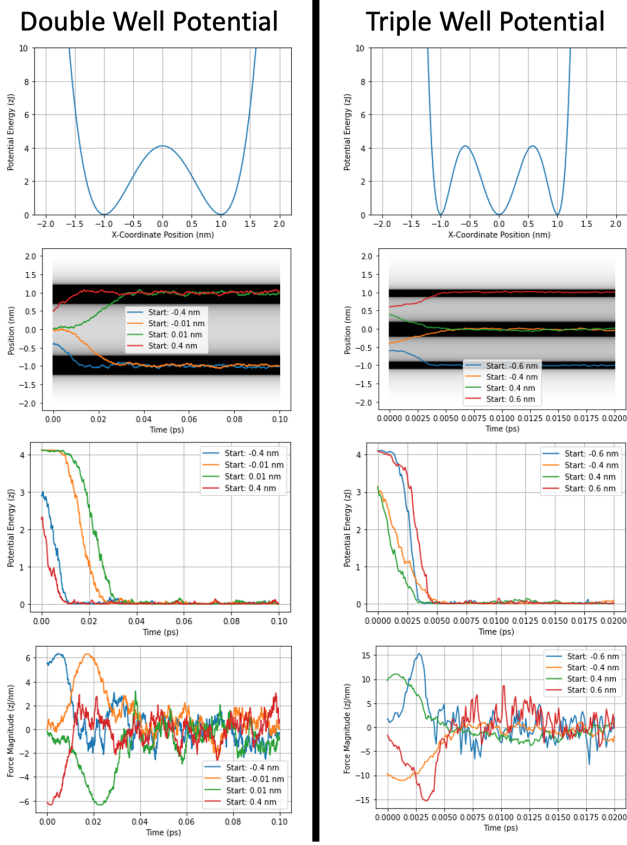


**Figure 1:** A comparison of various Brownian particles at different starting points on either double- or triple-well 1D potential energy surfaces. Top: potential energies as a function of x-coordinate. Top Middle: Brownian particles at various starting positions gravitating towards local minimal energy wells with respect to x position. Bottom Middle: Potential Energy convergence of particles. Bottom: Force vector magnitude of particles through simulation time.

functions. Figure 1 shows the double- and triple-well potentials as well as the behavior of a Brownian particle placed at various starting points (with corresponding energy and force magnitude assessments). Note that Brownian particles quickly gravitate towards the nearest potential energy minimum and are trapped in that position for the foreseeable future, with only a very small likelihood of bouncing to the other potential energy minimum for all but the smallest well heights.

## 2.2 Umbrella Sampling

Based on the dynamics of Brownian particles in rapidly reaching a minimum on the potential energy surface, we observe that we may not adequately sample at higher potential regimes to accurately assess the free energy of the system. Umbrella sampling seeks to correct this through a potential energy biasing across a series of small binned ranges across x-coordinates. This bias typically follows

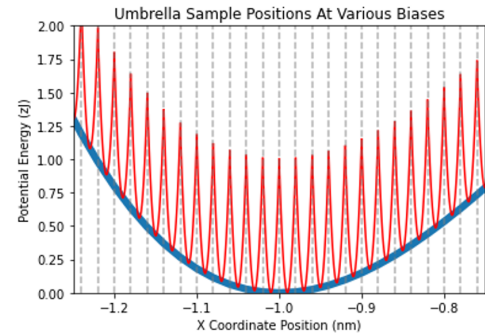


**Figure 2:** A simple division of umbrella biases with respect to a local double-well potential energy landscape.

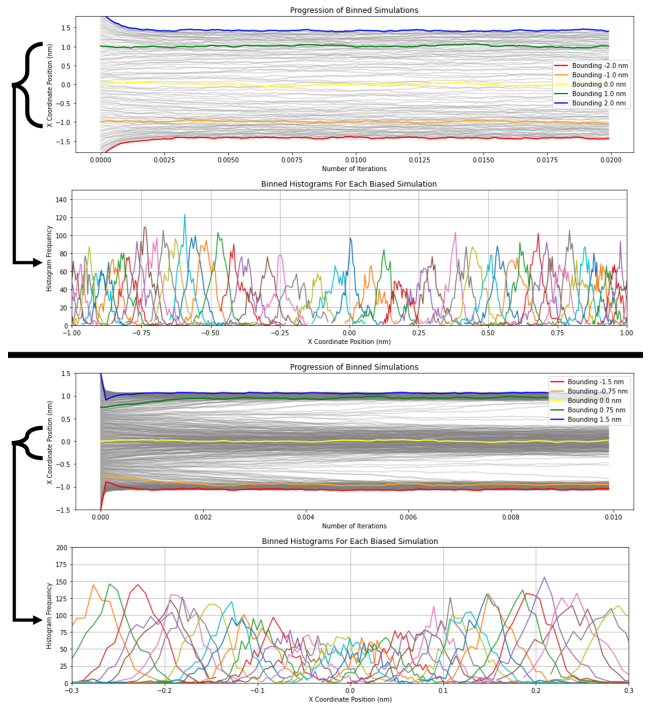


**Figure 3:** Top: Biased trajectories of particles over a simulation run for a double-well potential. Top middle: Binned histograms of particles for a given biased trajectory on a double-well potential. Bottom middle: Biased trajectories of particles over a simulation run for a triple-well potential. Bottom: Binned histograms of particles for a given biased trajectory on a triple-well potential.

a quadratic (or harmonic) formulation, which may be expressed as

$$U_{bias}(x; x_{bias}) = \frac{1}{2} C k_B (x - x_{bias})^2$$

where  $C$  is an arbitrary constant and  $x_{bias}$  will be the left-hand side of our binned region [3]. Each pre-specified bin therefore receives a different biasing equation. Figure 2 demonstrates this biasing on narrow bins across a small slice of the potential energy landscape.

Supposing a set of  $N$  bins generating  $N$  full MD simulations, we specify the bins across our reaction coordinate  $x$  as  $\{x_0, \dots, x_N\}$ , with bin widths specified as  $x_{i+1} - x_i = \frac{x_N - x_0}{N}$ . We can select the proper number of bins across the reaction coordinate by analyzing the degree of overlap among binned regions after performing the MD simulation [4]. Since stitching together individual simulations relies on reaction coordinate overlap between adjacent bins, we must adjust the corresponding number of bins based on this principle. Figure 3 demonstrates this process in the case of both double-well and triple-well potentials. Note that there is significant overlap between adjacent bins within the histogram. One other observation is necessary: the harmonic biasing of the potential energy is not always sufficient to overcome a large potential energy gradient. Therefore we observe that in both the double-well and triple-well potentials that for bins at far extrema from an energy minimum, the particle is inevitably drawn outside of the fixed boundary despite the strong biasing. This can be accounted for by either narrowing the observed reaction coordinate range or by increasing the constant  $C$  to further bias simulations with high potential energy gradients.

### 2.3 WHAM and UWHAM/MBAR

After sampling across all individually biased regimes, we must now unbias each bin and stitch individual samples together, effectively combining the free energy contribution of each simulation towards a greater whole. This can be quite a difficult prospect, especially for a large number of bins. All approaches are based on the convergence of the Helmholtz free energy values at each bin. The first approach devised to accomplish the unbiasing and stitching was the weighted histogram analysis method (WHAM) [5]. This approach formulates the problem in terms of a nonlinear optimization, expressed in the form

$$\begin{aligned} \min_{\{A_0=0, A_1, \dots, A_N\}} \quad & \sigma^2 = \sum_{k=1}^n C_k^2(x) \sigma_k^2 \\ \text{w.r.t. } & \sum_{k=1}^n C_k(x) = 1 \end{aligned}$$

where

$$C_k(x) = \frac{n_k / [\epsilon_k(x) \tilde{H}_k(x) e^{-2\beta(A_k - A_0)} e^{2\beta U_{k,bias}(x - x_{k,bias})}]}{\sum_{j=1}^n n_j / [\epsilon_j(x) \tilde{H}_j(x) e^{-2\beta(A_j - A_0)} e^{2\beta U_{j,bias}(x - x_{j,bias})}]}$$

and

$$\sigma_k^2 = e^{-2\beta(A_k - A_0)} e^{2\beta U_{k,bias}(x, x_{k,bias})} [\epsilon_k(x) \tilde{H}_k(x) / (n_k \Delta x)].$$

Within this nonlinear optimization, we have  $x$  as the desired reaction coordinate,  $\{A_0, \dots, A_N\}$  as the Helmholtz free energies at each time step (arbitrarily setting  $A_0 = 0$  since free energy calculations are relative),  $n_k$  represents the total number of samples taken within the bin located at  $x_{k,bias}$ ,  $\epsilon_k(x)$  represents the deviation of a reaction coordinate from the initial  $x_{k,bias}$ ,  $\tilde{H}_k(x)$  represents the histogram frequency count at each point within a simulated bin, and  $\Delta x$  is the bin width [6].

This is a feasible method for stitching together a smaller number of bins, this method quickly runs into issues at larger numbers of bins. While we did write an implementation of WHAM in the above form, we could under no circumstances reach numerical

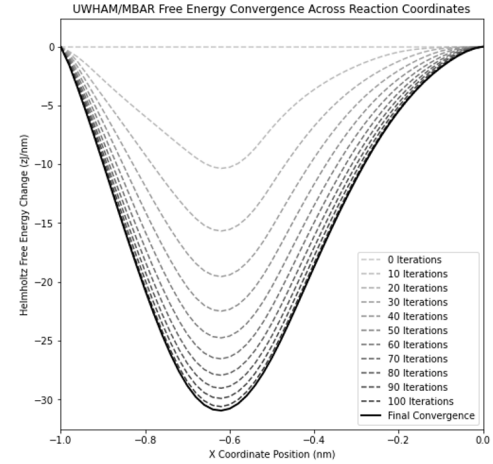


**Figure 4: Convergence of WHAM for a double-well potential with respect to changes in Helmholtz free energy.**

convergence with this approach. We therefore opt for a far simpler implementation that bypasses histogram partitioning within bins, and is known as unbinned weighted histogram analysis method (UWHAM) [7]. It has been shown that UWHAM is functionally equivalent to multistate Bennett acceptance ratio (MBAR) [8], therefore we shall use these terms interchangeably. UWHAM/MBAR takes the relatively far more simple update procedure as follows:

$$\hat{A}_k \leftarrow -\beta^{-1} \ln \left[ \sum_{j=1}^k \sum_{n=1}^{n_j} \frac{e^{-\beta U_{j,bias}}}{\sum_{k=1}^N [N_k e^{\beta(\hat{A}_k - U_{k,bias})}]} \right] \forall \hat{A}_k.$$

We proceed with this update procedure until  $\sum \hat{A}_k < \varepsilon$  for some pre-specified convergence criterion  $\varepsilon$ . This formulation has a number of benefits. It is easier to implement, it converges more rapidly, and it can handle even a large number of bins. Figure 4 demonstrates the convergence process for UWHAM with respect to step changes in Helmholtz free energy across the reaction coordinate. We see that after starting at  $\hat{A}_i = 0 \forall \hat{A}_i$ , in roughly 100 iterations of the UWHAM updates we reach a suitable convergence to a smooth free energy surface. Based on a handful of manual tests, it appears that while double-well and triple well potential convergence with UWHAM appear to follow  $O(n^3)$  complexity where  $n$  is the number of bins spanning the simulation space, the triple-well potential takes roughly five times more iterations to converge to an identical  $\varepsilon$  as its double-well counterpart. This suggests some relationship between the complexity of the underlying potential energy surface and the number of iterations required for free energy convergence, however the nature of this relationship is not entirely clear and warrants further inquiry.

## 3 RESULTS

With our methods in hand and our implementation prepared, we now begin testing our double-well and triple-well potential with a variety of ranging pre-sets. We first change the well heights, then the well widths, and finally we change both simultaneously to allow for a concise description of the total Helmholtz free energy

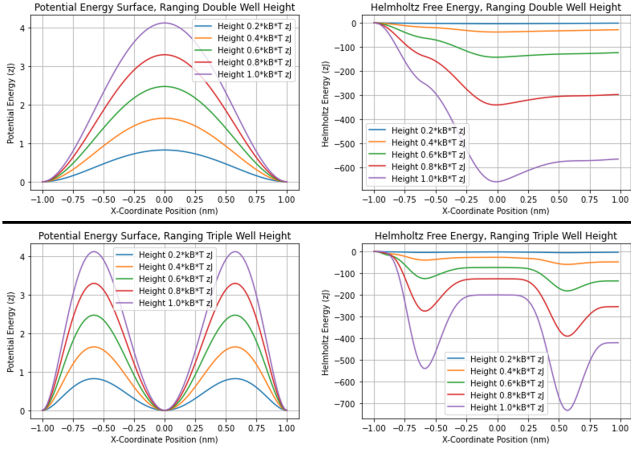


**Figure 5:** Top Left: double-well potential energy surfaces with varying heights. Top Right: corresponding Helmholtz free energies associated with varying heights of the double-well potential. Bottom Left: triple-well potential energy surfaces with varying heights. Bottom Right: corresponding Helmholtz free energies associated with varying heights of the triple-well potential.

change across our one-dimensional potential energy surface. We will consistently run our simulations across 100 evenly-sized bins, and process each simulation for a total of 1000 time steps (where  $dt = 0.0001$  ps), for a total duration of 0.1 ps.

We begin with an analysis of well heights. Figure 5 shows the results of testing at heights  $H = [0.2*k_B T, 0.4*k_B T, 0.6*k_B T, 0.8*k_B T, 1.0*k_B T]$  where  $k_B$  is once again the Boltzmann constant (held in zJ/K), temperature is held constant at  $T = 298$  Kelvin, and width is held constant at  $W = 2$  nm. We traverse across the reaction coordinate on the potential energy barrier from  $x = -1$  nm to  $x = 1$  nm. As expected, a larger height results in a corresponding larger change in Helmholtz free energy from one extreme to another. Interestingly, the free energy changes from the triple-well equation appear to be less overall, even though the heights are kept constant. One might attempt to explain this behavior by pointing out that at constant heights  $H$ ,

$$\int_{-W}^W U_2(x)dx > \int_{-W}^W U_3(x)dx > \dots > \int_{-W}^W U_n(x)dx.$$

We now move to an analysis of well widths. Figure 6 shows the results of testing at widths  $W_{tot} = [1, 2, 3, 4, 5, 6]$  with constant height  $H = k_B T$ . We once again traverse across the reaction coordinate on the potential energy barrier from  $x = -W/2$  nm to  $x = W/2$  nm. Surprisingly, we find that neither larger nor smaller free energy changes always result from a change in width. This may be due to two competing factors. A decrease in total displacement could be responsible for a lower free energy. The trade-off comes from a greater force required to overcome the potential energy barrier; that is, a decrease in  $W$  leads to an increase in  $\max(\frac{dU(x)}{dx})$  even when  $H$  is kept constant. For the double-well and triple well potentials, the greatest total change in Helmholtz free energy was the result of well distances of 2 nm and 4 nm, respectively.

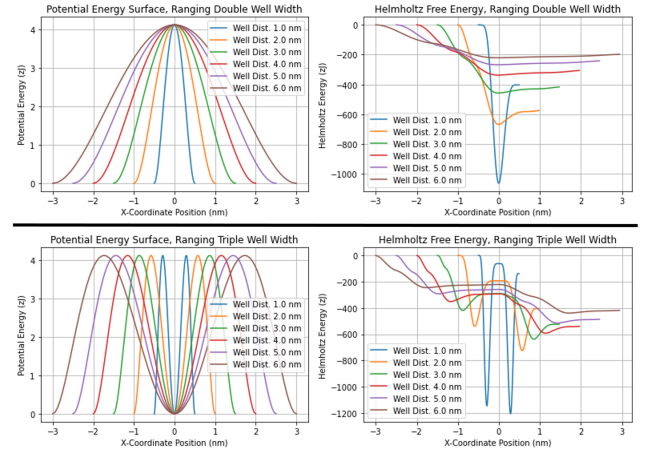


**Figure 6:** Top Left: double-well potential energy surfaces with varying widths. Top Right: corresponding Helmholtz free energies associated with varying widths of the double-well potential. Bottom Left: triple-well potential energy surfaces with varying widths. Bottom Right: corresponding Helmholtz free energies associated with varying widths of the triple-well potential.

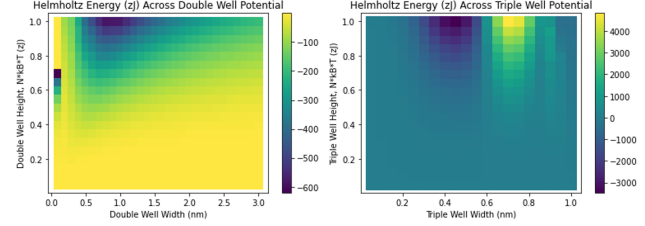


**Figure 7:** Left: total Helmholtz free energy change for a double-well potential with simultaneous changes in well height and width. Right: total Helmholtz free energy change for a triple-well potential with simultaneous changes in well height and width.

We close by analyzing the total changes in Helmholtz free energy with respect to simultaneous changes in both well height and width. Figure 7 demonstrates this idea on the double- and triple-well potentials. We generate a mesh that runs from  $H = [0.05*k_B T, \dots, 1.0*k_B T]$  and  $W = [0.1nm, \dots, 3.0nm]$  for the double-well potential and  $H = [0.05 * k_B T, \dots, 1.0 * k_B T]$  and  $W = [0.05nm, \dots, 1.0nm]$  for the triple-well potential. These regions were carefully selected such that numerical overflows could not occur either during the MD simulation or during the UWHAM convergence process. Any further outside this region and numerical instability would quickly cause poor convergence or no convergence. This problem with numerical stability made classical WHAM intractable, and UWHAM tractable only within narrow regimes. For the simulations that we were able to run, we see some interesting behaviors emerge. As we might expect, low well heights imply a very small change in total free energy, even at much wider widths. At greater heights, the results are more difficult to interpret. It is particularly unusual to see a rapid shift in

free energy changes at higher height values along the triple-well potential. We are unsure of how or why this behavior occurs, and would welcome an explanation from anyone so inclined.

## 4 CONCLUSION AND FUTURE WORK

We have now explained the methodology of umbrella sampling and UWHAM, demonstrated a working implementation, and shown the resulting free energy calculations on a double- and triple-well potential energy surface across various parameter sweeps. In particular, we explore how changes to the height and width of our potential energy surface impact the overall change in the free energy landscape.

While this survey has already unearthed a number of interesting results, there are a number of other avenues that might be explored in the future. This could include demonstrating how changing the number of bins improves free energy accuracy across a reaction coordinate, or how running each MD simulation for a longer time period can also improve free energy accuracy. While we chose to run for a constant 0.1 picoseconds per simulation, one need not necessarily run each simulation for the same duration. In other words, a particle with a set potential energy bias which explore a wider range within a reaction coordinate may require more or less time steps than a particle with a set potential energy bias on

a narrow range within a reaction coordinate. In cases where the MD simulation is itself the rate-limiting step, after some initial MD burn-in one might incorporate Thompson sampling to actively select which particle to continue simulating in order to optimally reduce deviation during UWHAM unbiasing and stitching. We hope to explore some of these techniques in the future, or look forward to reading about others having done so.

## REFERENCES

- [1] Tamar Schlick. *Molecular modeling and simulation: an interdisciplinary guide: an interdisciplinary guide*, volume 21. Springer Science & Business Media, 2010.
- [2] Hyun Kyung Shin, Changho Kim, Peter Talkner, and Eok Kyun Lee. Brownian motion from molecular dynamics. *Chemical Physics*, 375(2-3):316–326, 2010.
- [3] Johannes Kästner. Umbrella sampling. *Wiley Interdisciplinary Reviews: Computational Molecular Science*, 1(6):932–942, 2011.
- [4] Benoît Roux. The calculation of the potential of mean force using computer simulations. *Computer physics communications*, 91(1-3):275–282, 1995.
- [5] Shankar Kumar, John M Rosenberg, Djamal Bouzida, Robert H Swendsen, and Peter A Kollman. The weighted histogram analysis method for free-energy calculations on biomolecules. i. the method. *Journal of computational chemistry*, 13(8):1011–1021, 1992.
- [6] Bin W Zhang, Junchao Xia, Zhiqiang Tan, and Ronald M Levy. A stochastic solution to the unbinned wham equations. *The journal of physical chemistry letters*, 6(19):3834–3840, 2015.
- [7] Bin W Zhang, Shima Arasteh, and Ronald M Levy. the uwham and swham software package. *Scientific reports*, 9(1):1–9, 2019.
- [8] Michael R Shirts. Reweighting from the mixture distribution as a better way to describe the multistate bennett acceptance ratio. *arXiv preprint arXiv:1704.00891*, 2017.